

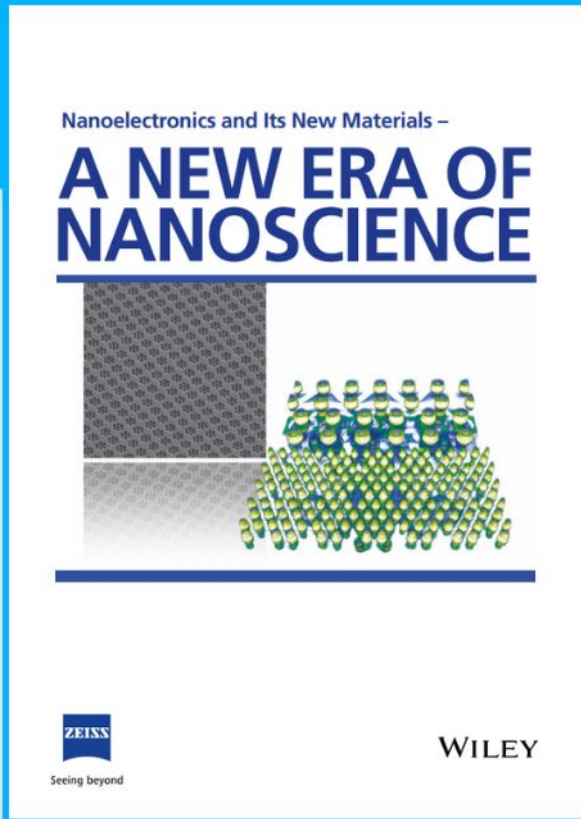


Nanoelectronics and Its New Materials – A NEW ERA OF NANOSCIENCE

Discover the recent advances in electronics research and fundamental nanoscience.

Nanotechnology has become the driving force behind breakthroughs in engineering, materials science, physics, chemistry, and biological sciences. In this compendium, we delve into a wide range of novel applications that highlight recent advances in electronics research and fundamental nanoscience. From surface analysis and defect detection to tailored optical functionality and transparent nanowire electrodes, this eBook covers key topics that will revolutionize the future of electronics.

To get your hands on this valuable resource and unleash the power of nanotechnology, simply download the eBook now. Stay ahead of the curve and embrace the future of electronics with nanoscience as your guide.



Seeing beyond

WILEY

Reversible Electronic Patterning of a Dynamically Responsive Hydrogel Medium

Chen Yang, Yi Liu, Many Wang, Hui Hu, Zhongtao Zhao, Hongbing Deng, Gregory F. Payne,* and Xiaowen Shi*

A dynamically responsive hydrogel medium is prepared from two self-assembling components, a polysaccharide (chitosan) and a surfactant (sodium dodecyl sulfate; SDS). It is shown that this medium can be patterned using an electrode “pen” to reconfigure supramolecular structure: cathodic writing induces neutral chitosan chains to form a crystalline network, while anodic writing generates cationic chitosan chains that electrostatically crosslink with anionic SDS micelles. Both supramolecular structures are re-configurable and each is stabilized by structure-induced shifts in chitosan’s pKa, thus electronically written patterns can be erased, new patterns can be written, and patterns can be written in three dimensions. Further, it is shown that NaCl-induced morphological transitions of the SDS micelles allow patterns to be reversibly concealed or revealed. To demonstrate the versatility of this medium for information storage, a quick response (QR) code is electronically written and it is shown that this code can be recognized by a standard cellphone app. This QR code can be concealed by making the medium opaque (i.e., by obscuring the pattern) or by making the pattern evanescent (i.e., by making pattern invisible). Overall, this work demonstrates that a dynamically responsive medium composed of simple, safe and sustainable components can be reversibly patterned with spatial and quantitative control using top-down electronic inputs.

1. Introduction

Biological polymers are known to undergo precise and complementary intermolecular interactions (e.g., hydrogen bonding) that enable self-assembly.^[1–3] In many cases, the supramolecular structure of self-assembling systems cannot be predicted based solely on the internal information coded in the biopolymer’s sequence. In these cases, the emergent supramolecule structure also depends on external, contextual information (i.e., stimuli).^[4,5] For instance, biology achieves incredible morphological diversity from a comparatively small set of structural building blocks (e.g., collagen, cellulose, and chitin) by controlling how these building blocks are interconnected.^[6,7] Presumably, the modularity and versatility of these “dynamic patterning modules”^[8–10] confer efficiencies for biology, while also providing individual organisms with mechanisms to learn and adapt to their local conditions.^[11]

In technological studies, dynamically responsive materials systems^[12–16] offer

the opportunity to control bottom-up self-assembly by the precise addition of external information (i.e., top-down cues) that are often imposed using stamping^[17–18] or printing^[19] methods. In many such studies, synthetic polymers are selected that possess intrinsic stimuli-responsive properties (e.g., thermal-responsiveness)^[13] or are synthesized to have moieties that confer dynamically responsive properties (e.g., pH-dependent metal chelating groups).^[18] Such responsive hydrogel materials are being investigated for a range of applications that include anti-counterfeiting,^[20–21] information encryption,^[22–26] and intelligent bionics.^[27]

Here, we investigated a dynamically responsive medium composed of two components: the aminopolysaccharide chitosan and the anionic surfactant sodium dodecyl sulfate (SDS). As illustrated in **Scheme 1a**, chitosan is pH-responsive and self-assembling,^[28–31] while SDS self-assembles into micelles. At high pH, chitosan’s amines are deprotonated, the chains are neutral and can self-assemble with inter-chain associations forming the crystalline network junctions (i.e., crosslinks);^[32–33] we designate this supramolecular network state as [(Chit)]. Under such neutral conditions, there are limited interactions between the crystalline chitosan network and the SDS micelles, and the supramolecular state of such a neutral mixture is designated [(Chit)+(SDS)].

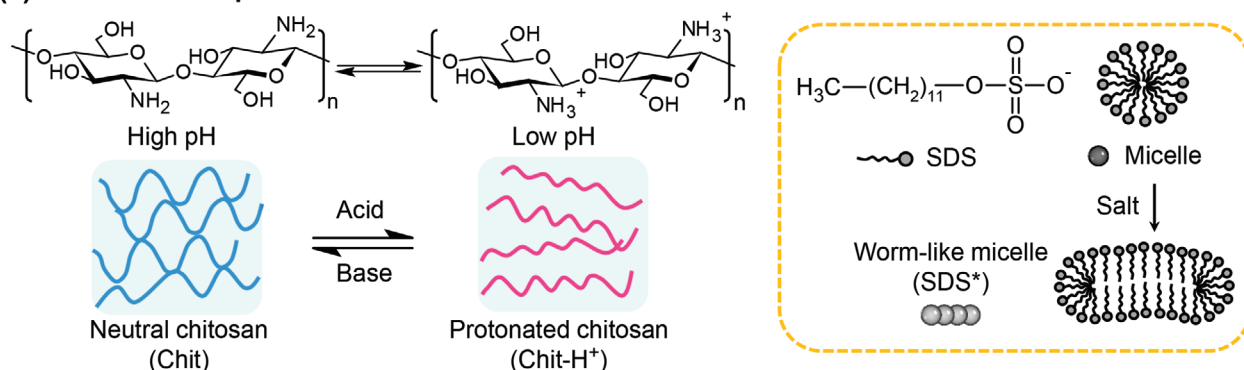
C. Yang, M. Wang, H. Hu, Z. Zhao, H. Deng, X. Shi
School of Resource and Environmental Science
Hubei Engineering Center of Natural Polymers-Based Medical Materials
Hubei Biomass-Resource Chemistry and Environmental Biotechnology
Key Laboratory
Hubei International Scientific and Technological Cooperation Base of
Sustainable Resource and Energy
Wuhan University
Wuhan 430079, China
E-mail: shixw@whu.edu.cn
Y. Liu, G. F. Payne
Institute for Bioscience and Biotechnology Research and Robert E. Fischell
Institute for Biomedical Devices
University of Maryland
College Park, MD 20742, USA
E-mail: gpayne@umd.edu

The ORCID identification number(s) for the author(s) of this article can be found under <https://doi.org/10.1002/adfm.202302549>

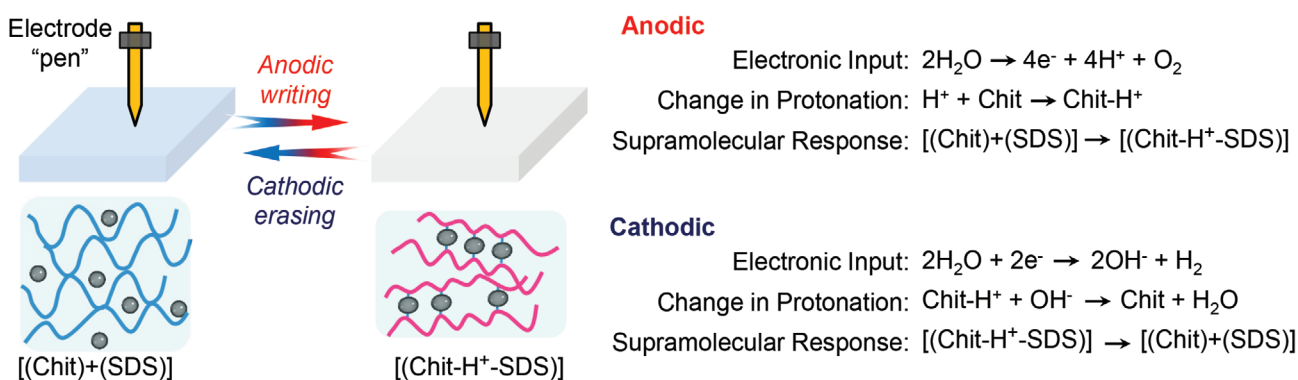
© 2023 The Authors. Advanced Functional Materials published by Wiley-VCH GmbH. This is an open access article under the terms of the Creative Commons Attribution-NonCommercial-NoDerivs License, which permits use and distribution in any medium, provided the original work is properly cited, the use is non-commercial and no modifications or adaptations are made.

DOI: 10.1002/adfm.202302549

(a) Molecular to Supramolecular Structure



(b) Electrochemical Writing/Erasing



Scheme 1. Schematics illustrating: a) chitosan's pH-responsiveness and SDS's self-assembly; b) electrochemical writing and erasing of information to the chitosan-SDS medium.

At low pH, chitosan's amines are protonated making chitosan a cationic polyelectrolyte: the chains are dissociated from the crystalline network junctions and undergo electrostatic crosslinking with SDS micelles to form a supramolecular state designated $[(\text{Chit-H}^+-\text{SDS})]$. Previous studies have shown that pH changes can cue reversible reconfigurations between the $[(\text{Chit})+(\text{SDS})]$ and $[(\text{Chit-H}^+-\text{SDS})]$ supramolecular states.^[34–36]

We report that an electrode "pen" can reversibly and spatially selectively reconfigure these supramolecular states and thus write information to this dynamically responsive chitosan-SDS medium. Scheme 1b shows that when the electrode imposes transient anodic inputs, the electrolytic reactions provide the acidic cues that induce the medium to respond by reconfiguring from $[(\text{Chit})+(\text{SDS})]$ to $[(\text{Chit-H}^+-\text{SDS})]$ states. Alternatively, cathodic inputs provide the transient basic cues that induce the network to reconfigure from $[(\text{Chit-H}^+-\text{SDS})]$ to $[(\text{Chit})+(\text{SDS})]$ states. Importantly, the patterns that are electronically written into the medium involve changes in supramolecular structure (not changes in composition or covalent bonding) and thus are reversible (i.e., the pattern can be erased). Also important, is that the pattern generated by the imposed transient electronic inputs persists after the pH gradient has dissipated because the supramolecular network structures are stabilized by structure-induced shifts in chitosan's pKa.^[33,37] Specifically, the pKa for chitosan's amines is shifted downward in the crystalline network junctions and shifted upward when engaged in electrostatic

crosslinking with SDS. We demonstrate that by combining anodic and cathodic writing, it is possible to pattern the medium in three dimensions which suggests that this dynamic medium can be used as a re-writable 3D memory.

In addition, Scheme 1a shows that SDS can undergo reversible structural transitions, and we show that these supramolecular transitions can be used to conceal and reveal the information written into the chitosan-SDS medium. Specifically, SDS can undergo salt-induced transitions from spherical micelles (designated SDS) to worm-like micelles (designated SDS*) that alter the medium's transparency. As a simple demonstration, we generated a quick response (QR) code that is readable using a standard cellphone app but can be reversibly concealed. QR codes are commonly used in proof-of-concept studies to demonstrate that information can be stored in a medium and can be purposefully concealed and revealed. In most such studies, a "permanent" QR code is created that can be concealed and revealed based on specific optical properties of the materials used (e.g., fluorescence excitation/emission wavelengths^[21,38] or birefringence^[39]). In our studies, we electronically pattern the QR code onto the dynamically responsive chitosan-SDS medium and show that it can be reversibly concealed using two mechanisms: by obscuring the pattern or by making the pattern invisible (evanescent). We show that a concealed QR code can be updated by adding or deleting information and that evanescent portions of the QR code can be reversibly revealed. Overall, this report

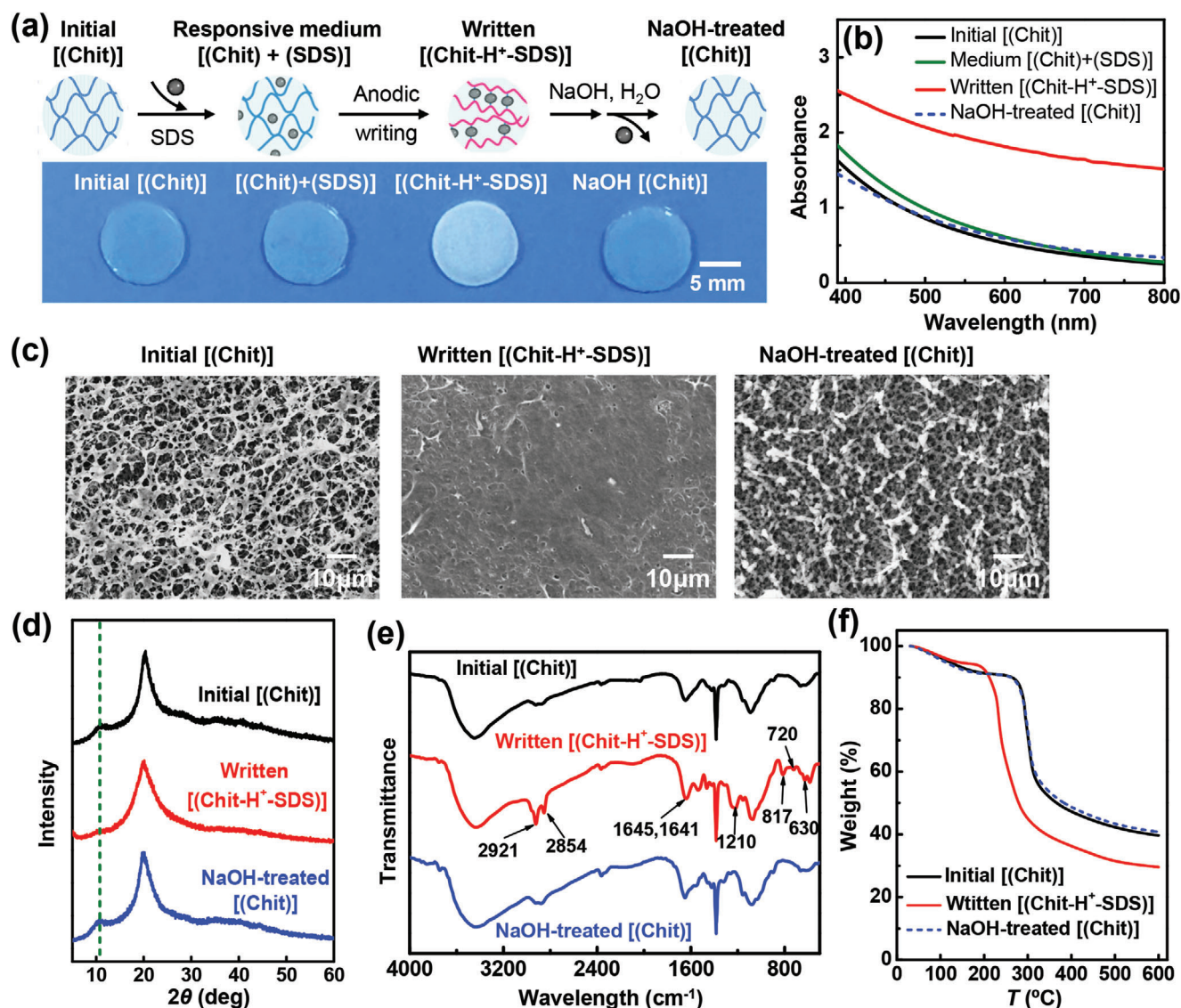


Figure 1. Initial evidence that anodic writing can reconfigure [(Chit)+(SDS)] to [(Chit-H⁺-SDS)] supramolecular state. Optical evidence for reconfiguration is provided by a) photograph, and b) spectrophotometric measurements. c) FE-SEM images suggest SDS confers a different microstructure for the [(Chit-H⁺-SDS)] versus [(Chit)] networks. Chemical evidence for different crosslinking interactions and supramolecular structures for the chitosan-SDS medium: d) XRD, e) FT-IR, and f) TGA. Additional evidence is provided in Figure S1 (Supporting Information).

shows the coupling of bottom-up and top-down information to write/erase/conceal/reveal information using; i) a medium that is simple (composed of chitosan, SDS, salt and water), sustainable (relying on two biologically derived materials), and safe (potentially edible); and ii) top-down electronic cues that can be imposed rapidly, safely (low voltages; ≈ 10 V), and without the need for reagents.

2. Results and Discussion

2.1. Anodic Inputs Reconfigure Hierarchical Structure

Initially, we prepared a relatively concentrated chitosan solution (3%; pH 5–6) with stoichiometric amounts of HCl. This concentrated solution was poured into a petri dish to a thickness

of 1 mm, neutralized with 1 M NaOH and rinsed with deionized water. As schematically shown in **Figure 1a**, this neutralized [(Chit)] hydrogel was immersed in SDS solution (0.2 M; pH ≈ 10 ; for 1 h) to obtain our dynamically responsive medium designated [(Chit)+(SDS)]. To write onto this medium, we used a platinum wire (diameter 0.8 mm) as an electrode pen. The electrode's writing movements were controlled by a mechanical arm (Ultimaker 2 Go, Beijing Hesheng Technology Co., Ltd.) with a writing speed 5 mm s^{-1} . For electrical writing, we used the Digital Source-meter (2450, Keithley, USA), and connected the wire pen as the anode and a platinum electrode as the cathode. After writing, the film was washed with water to remove loosely bound SDS micelles.

Figure 1a shows that the initial [(Chit)] hydrogel and the [(Chit)+(SDS)] medium were optically clear but became opaque after anodic writing (6 strokes, using 3 mA for a total of 6 min)

and water washing (further details of anodic writing are discussed below). As discussed, the pen's transient anodic signal is expected to create the local low pH conditions that induce chitosan to reconfigure from a network that is physically crosslinked through crystalline network junctions to a network with disassembled chitosan chains that are electrostatically crosslinked by SDS micelles. Presumably, the [(Chit-H⁺-SDS)] hydrogel is opaque because of the SDS micelles that are engaged in electrostatic interactions with chitosan are deformed.^[33,40] When this written gel was immersed in base (1 M NaOH; 2 min) and then washed with water, Figure 1a shows it returns to its clear appearance consistent with the initial [(Chit)] state. Figure 1b provides quantitative spectrophotometric evidence for the changes in optical properties of these films. The absorbance of the written [(Chit-H⁺-SDS)] hydrogel is much higher than others, consistent with the photographs in Figure 1a.

The FE-SEM (field emission scanning electron microscope) images in Figure 1c show that the initial neutralized chitosan hydrogel [(Chit)] has a loose, porous structure (pore size $2.5 \pm 0.6 \mu\text{m}$), while the electrostatically cross-linked [(Chit-H⁺-SDS)] hydrogel appears dense (pore size $1.1 \pm 0.3 \mu\text{m}$). After NaOH treatment and water washing (24 h), the SEM image (pore size $1.7 \pm 0.4 \mu\text{m}$) in Figure 1c appears similar to the initial [(Chit)] which suggests water washing can remove SDS micelles that are not electrostatically crosslinked with chitosan. These observations are consistent with previous reports.^[34]

Various chemical approaches were used to demonstrate that anodic writing can reconfigure the crosslinking interactions and supramolecular structure of the chitosan-SDS medium. The X-ray diffractograms (XRD) in Figure 1d show a reflection at 2θ value of 10.8° for the initial [(Chit)] and NaOH-treated [(Chit)] hydrogel films but not for the [(Chit-H⁺-SDS)] hydrogel. This result is consistent with a crystalline network for the [(Chit)] films and the loss of crystallinity for the SDS crosslinked film.^[41]

Figure 1e shows FT-IR spectra for the various films. The absorption peak at 1645 cm^{-1} is assigned to the characteristic peak of C=O stretching vibration (amide I) of chitosan's *N*-acetyl groups. The absorption peaks at 1641 and 1210 cm^{-1} (SO₂ stretching), 817 and 720 cm^{-1} (S–O–C asymmetric and symmetric stretching), 630 cm^{-1} (SO₃ flexion), and $3000\text{--}2800 \text{ cm}^{-1}$ (C–H stretching regions) are assigned to the characteristic peaks of SDS.^[42] The differences in the spectra for these three films indicate that water washing can remove SDS from the neutralized chitosan film, but water washing cannot remove SDS from the electrostatically crosslinked [(Chit-H⁺-SDS)] hydrogel film.

Figure 1f shows the thermogravimetric analysis (TGA) for these three hydrogels while derivative thermogravimetry graphs are shown in the Supporting Information (Figure S1). The results for the initial [(Chit)] and the NaOH-treated [(Chit)] films were very similar while the result for the [(Chit-H⁺-SDS)] hydrogel appears to be less stable. Possibly the difference in thermal stability may be related to the differences in crystallinity.^[43]

In conclusion, the results in Figure 1 (and Figure S1, Supporting Information) provide initial evidence that anodic writing can reconfigure the crosslinking interactions and supramolecular organization of the chitosan–SDS medium to convert an initially crystalline network into an electrostatically crosslinked [(Chit-H⁺-SDS)] network. This reconfiguration is reversible as the crystalline network can be regenerated by base treatment.^[35]

2.2. Electronic Control of Supramolecular Reconfiguration

2.2.1. Anodic Writing

To demonstrate that anodic writing can be used to controllably pattern the chitosan-SDS medium we first examined the medium's response to the intensity of the imposed electrical input. Experimentally, Figure 2a shows that we placed the electrode pen on the surface of the medium and imposed inputs of different intensities by varying either the applied anodic current or the time. The photographs of the spots and corresponding radius-time plots show that the size of the patterned spot increased with electrical input intensity.

Previous studies in which a stationary electrode pen was used to impose electrical inputs to induce a pH-mediated supramolecular reconfiguration used a moving front model^[44] as a theoretical framework to suggest how structural outputs should be correlated to electrical inputs.^[45] Briefly, the model assumes: i) the charge transfer measured at the electrode ($Q = \int idt$) is equal to the proton transfer from chitosan (the solution has no other buffers); ii) proton transfer reactions are rapid relative to diffusion such that the electrode-induced pH change travels as a front; iii) the association/dissociation of neutral chitosan chains is rapid such that the pH front and assembly/dis-assembly front are co-localized. The model and the previous experimental results showed a linear correlation between the radius of the semi-circular spot and $(Q_{A,S}/c)^{1/3}$ where $Q_{A,S}$ is the anodic charge transferred during spotting ($Q_{A,S} = \int idt$) and c is chitosan concentration in the medium. The plot at the right in Figure 2a shows a similar linear correlation with a slope of 0.06 which is comparable to value observed of 0.07 that was observed in previous studies.^[45] Thus, the moving front model provides a quantitative framework relating the electric input (Q) to the extent of structural response (radius or depth of the change in supramolecular structure).

Next, we examined the ability to write patterns by moving the electrode pen across the [(Chit)+(SDS)] medium while applying an anodic current. To demonstrate the spatial selectivity for anodic writing, we wrote onto the medium using electrode pens of different diameters and imposed currents. As expected, Figure 2b shows the width of the line increased with either an increase in the pen's diameter or the applied current. To demonstrate that the written patterns are stable, we wrote a leaf pattern (4 strokes, 3 mA). This leaf-patterned hydrogel was stored in water at room temperature. The images in Figure 2c show the pattern is stable even after being stored wet for 60 days. This stability is believed to be due to the pKa shifts induced by the different localized interactions between the [(Chit)+(SDS)] and [(Chit-H⁺-SDS)] supramolecular structures.^[33,37] Specifically, chitosan's crystalline network junctions in [(Chit)+(SDS)] are stabilized by a structure-induced decrease in pKa (the neutral amine state is stabilized in the hydrophobic environment in the crystalline region), while the electrostatic crosslinking in [(Chit-H⁺-SDS)] shifts the pKa upward by a stabilization of the protonated amine state. This pKa difference allows for gradients in supramolecular structure to be stable over time.

To provide evidence that anodic writing offers a quantitatively controllable means to induce changes in intermolecular interactions and supramolecular structure, we examined correlations between the intensity of the imposed electrical input and

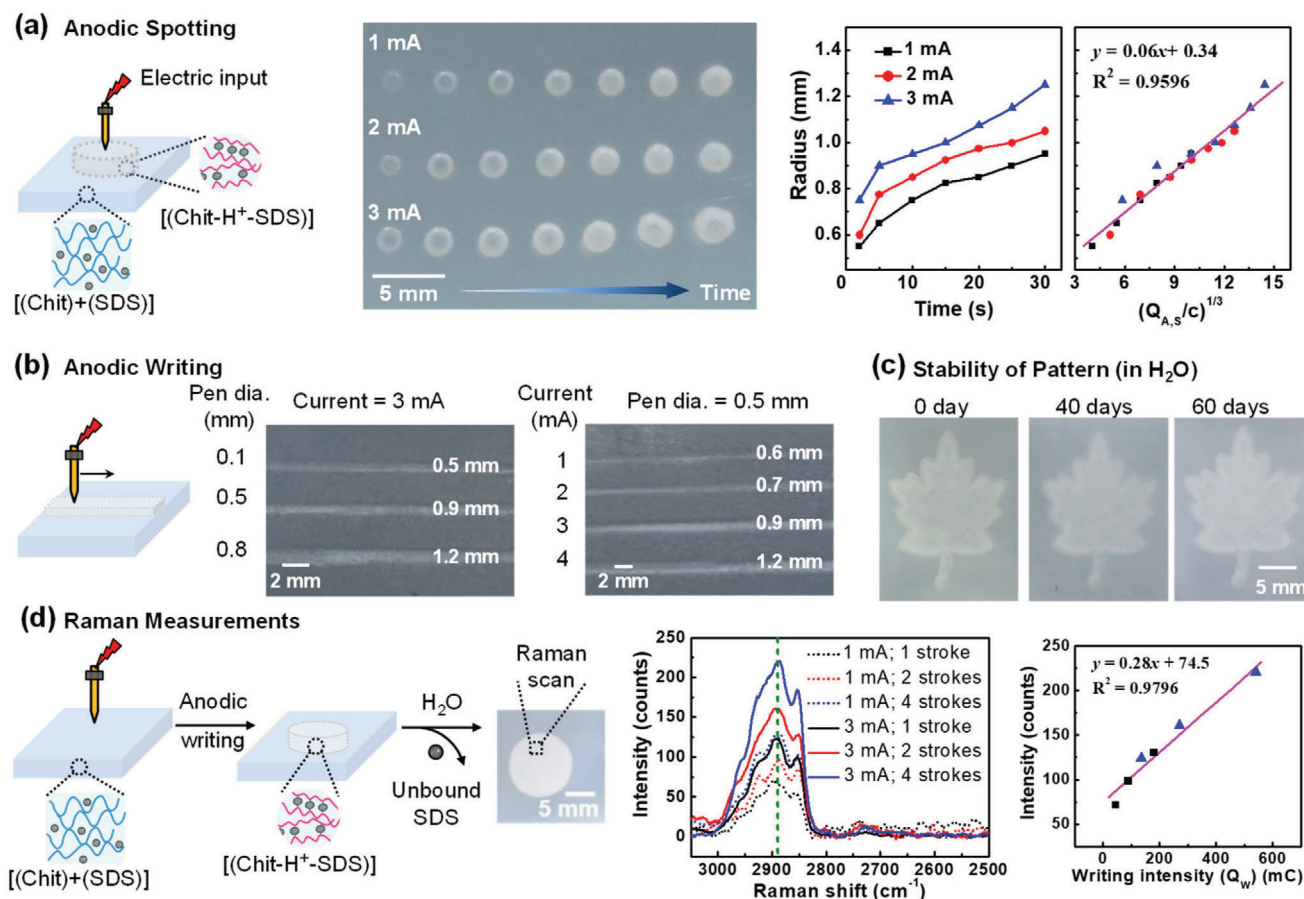


Figure 2. Electronic control of anodically induced reconfiguration of supramolecular structure. a) Anodic spotting. b) Anodic writing. c) Stability of written pattern in water. d) Raman measurements of electrostatically crosslinked chitosan-SDS hydrogel films.

the changes in structural output. Experimentally, as shown in Figure 2d, we wrote onto the medium using an electrode pen (diameter 0.8 mm), at a writing speed (v) of 5 mm s⁻¹ using different applied currents (i) and a different number of writing strokes (n) over the same region of length (l ; typically 225 mm). After writing the films were washed with water to remove unbound SDS micelles (i.e., micelles not engaged in electrostatic crosslinking interactions with chitosan). Figure S2a (Supporting Information) shows patterns written with different anodic writing intensities. The anodic writing intensity (Q_w) was quantified as:

$$Q_w = n \frac{i}{v} l \quad (1)$$

To quantify the output structural response, we used Raman spatial imaging.^[46–47] Specifically, we focused on the C–H stretching intensities (2800–3000 cm⁻¹),^[48–49] associated with SDS electrostatic crosslinks (note SDS micelles not engaged in electrostatic crosslinks were removed by water washing). For 2D imaging, we use heat maps where the output patterning intensity is quantified by the peak intensity at 2890 cm⁻¹ (Figure S2b in Supporting Information shows the 2D heat maps for regions patterned with different intensities). As illustrated by the spectra in Figure 2d, higher Raman intensities at 2890 cm⁻¹ were ob-

served for films written with greater anodic writing intensity. The averaged Raman spectra for regions patterned with different writing intensities are shown in the summary plot of Figure 2d that shows a linear increase in supramolecular structural outputs (i.e., SDS-mediated electrostatic crosslinking) with anodic writing intensity.

2.2.2. Cathodic Erasing

To demonstrate that cathodic inputs can be used to controllably erase the [(Chit-H⁺-SDS)] supramolecular structure, we first performed spotting studies with a stationary electrode to examine the films' response to the intensity of the imposed electrical input. Experimentally, Figure 3a shows that we initially prepared a rectangular [(Chit-H⁺-SDS)] film (30×18 mm) by anodically writing (2 strokes, 3 mA) on the surface of a [(Chit)+(SDS)] medium. Then, we placed the electrode pen on the surface of the [(Chit-H⁺-SDS)] film and imposed different cathodic electrical input intensities by varying either the applied cathodic current or the time for spotting. The photograph and corresponding radius-time plots in Figure 3a show that the size of the erased spot increased with electrical input intensity. Analogous to the results for anodic spotting (i.e., Figure 2a), the summary plot at the right in Figure 3a shows

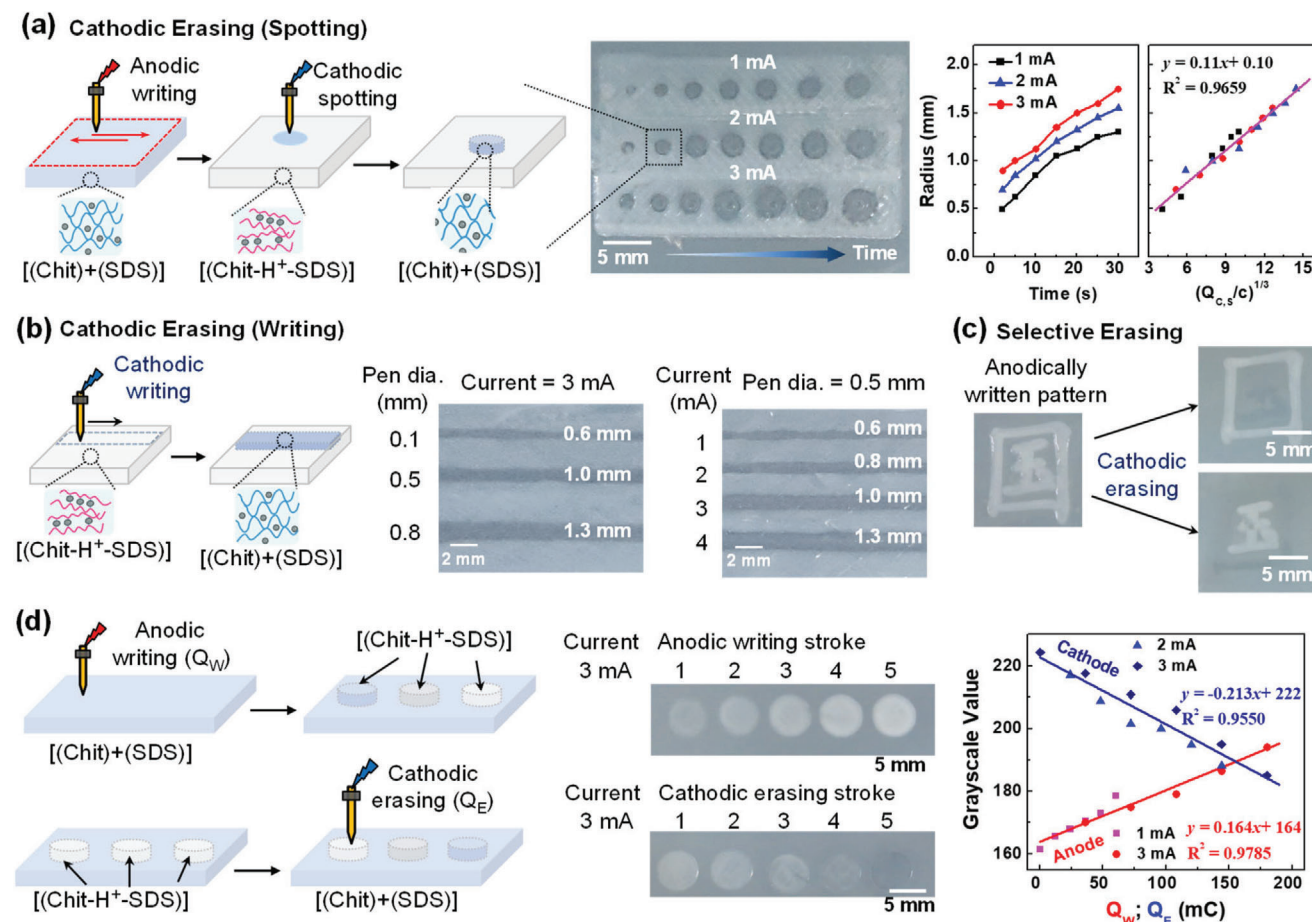


Figure 3. Electronic control of cathodically induced reconfiguration of supramolecular structure. a) Cathodic spotting (i.e., erasing). b) Cathodic writing (i.e., erasing). c) Selective erasing. d) Correlations between the observable indicators of structural changes and the intensity of electrical inputs for anodic writing and cathodic erasing.

a linear correlation between the erasure radius and intensity of the cathodic input for spotting ($Q_{C,S}/c^{1/3}$). It is interesting to note that the difference in slopes between these two plots (0.11 for cathodic erasing and 0.06 for anodic writing) is consistent with the qualitative observations that the anodic writing leads to a contraction of the medium.

To demonstrate that cathodic erasing is spatially controllable, we erased lines using electrodes of different diameters and cathodic input currents. As described above, we first anodically wrote on the medium to prepare a $[(\text{Chit-H}^+ \cdot \text{SDS})]$ film, and as illustrated in Figure 3b, we then cathodically erased lines using the electrode pen to reconfigure $[(\text{Chit-H}^+ \cdot \text{SDS})]$ regions back to $[(\text{Chit}) + (\text{SDS})]$. After rinsing with water to remove unbound SDS micelles, the photographs in Figure 3b show the width of the erased lines were greater when electrodes were used with larger diameters or higher cathodic current inputs (further visual evidence for cathodic erasing is shown in Figure S3, Supporting Information).

To further illustrate the spatial selectivity of cathodic erasing, we anodically wrote the Chinese character for “country” (国) onto a $[(\text{Chit}) + (\text{SDS})]$ medium (4 electrode writing strokes per written area, 3 mA) and then selectively erased portions of this character (4 strokes, 3 mA). The upper photograph in Figure 3c shows

that the internal portion of the character was erased, leaving the ancient character for “encircle” (口). The lower photograph in Figure 3c shows that the external portion of the character was erased, leaving the character for “jade” (玉). This qualitative demonstration illustrates the capability for spatially selective cathodic erasing.

To demonstrate that anodic writing and cathodic erasing are quantitatively controllable, we electronically wrote circular patterns and measured the grayscale values of these patterned regions using ImageJ. (Note: it was not possible to quantify cathodic erasing using Raman imaging as in Figure 2d because Raman mapping is surface sensitive.) For anodic writing, the upper scheme in Figure 3d shows that circular $[(\text{Chit-H}^+ \cdot \text{SDS})]$ patterns were written on the $[(\text{Chit}) + (\text{SDS})]$ medium with different anodic intensities (Q_W). The upper photographs and plot in Figure 3d show that the grayscale values of anodically written $[(\text{Chit-H}^+ \cdot \text{SDS})]$ regions increase linearly with Q_W . For cathodic erasing, the scheme at the bottom in Figure 3d shows that first we anodically wrote circular $[(\text{Chit-H}^+ \cdot \text{SDS})]$ patterns (5 strokes, 3 mA; $Q_W = 180$ mC), and then erased these patterns by converting these $[(\text{Chit-H}^+ \cdot \text{SDS})]$ regions into $[(\text{Chit}) + (\text{SDS})]$. The lower photographs and plot in Figure 3d show that the grayscale values of the erased regions decrease linearly with increasing erasing

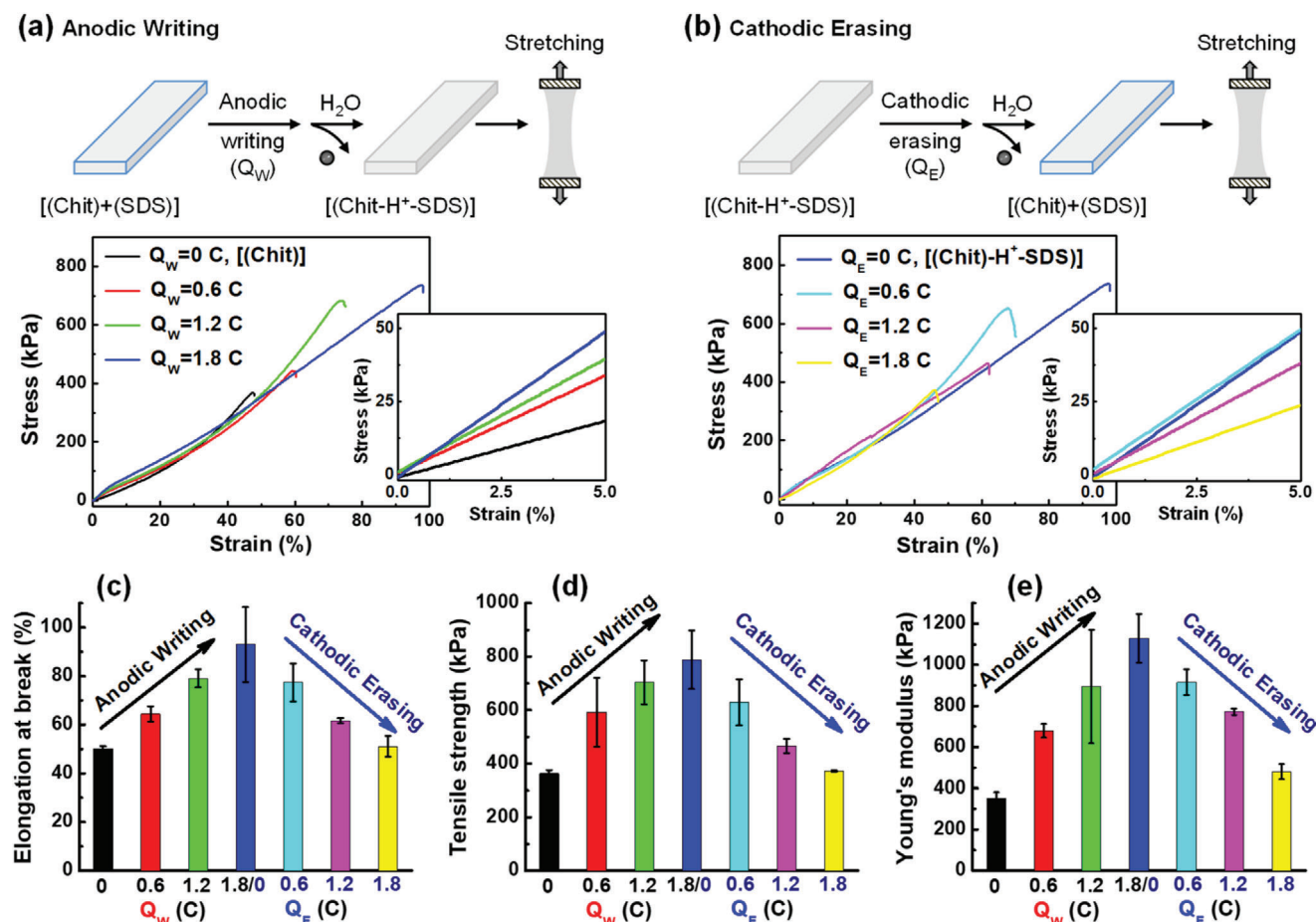


Figure 4. Functional evidence that electronic inputs that controllably reconfigure supramolecular structure, also controllably change mechanical properties. Schematic of mechanical testing of films after a) anodic writing and b) cathodic erasing. Correlations that show how electronic inputs for writing (Q_W) and erasing (Q_E) control; c) elongation at break, d) tensile strength, and e) Young's modulus.

intensity (Q_E). Together, the two lines in Figure 3d provide evidence that the hierarchical structure of the chitosan-SDS medium can be controllably reconfigured in response to imposed electrical input signals.

2.2.3. Functional Evidence for Reconfiguration

Previous studies^[34–35] showed that electrostatically crosslinked [(Chit-H⁺-SDS)] networks are denser and mechanically stronger than neutral [(Chit)+(SDS)] networks. We next performed experiments to demonstrate that electrode writing that is capable of reconfiguring supramolecular structure can also controllably alter mechanical properties. In studies illustrated in Figure 4a, we first prepared a neutral [(Chit)+(SDS)] medium and anodically wrote onto this medium with varying writing intensities Q_W . After washing the films with H₂O to remove the non-electrostatically bound SDS micelles, we measured the mechanical properties of the wet films (measurements were performed in air). The stress-strain curves in Figure 4a show that the film's mechanical properties were progressively enhanced when greater anodic writing

intensities were used to convert [(Chit)+(SDS)] into [(Chit-H⁺-SDS)].

In subsequent studies illustrated in Figure 4b, we prepared films in their [(Chit-H⁺-SDS)] network state by anodically writing onto the [(Chit)+(SDS)] medium with an intensity of $Q_W = 1.8$ C, and then we anodically erased this written [(Chit-H⁺-SDS)] film using varying cathodic erasing intensities Q_E . The stress-strain curves in Figure 4b show that the mechanical properties progressively decreased with an increase in the cathodic erasing intensity used to reconfigure the [(Chit-H⁺-SDS)] film back to the [(Chit)+(SDS)] state.

To quantitatively compare the effects of anodic writing and cathodic erasing on the chitosan-SDS medium's mechanical properties, we calculated three mechanical indices from the stress-strain curves. The elongation at break (Figure 4c), tensile strength (Figure 4d), and Young's modulus (Figure 4e) all show progressive increases with the increases of anodic writing intensity (Q_W), and progressive decreases with the increases in cathodic erasing intensity (Q_E). Further evidence that electrical inputs can controllably alter the medium's mechanical properties is provided in Table S1 and Figure S4 of the Supporting Information. In summary, the results in Figure 4 provide functional evidence that

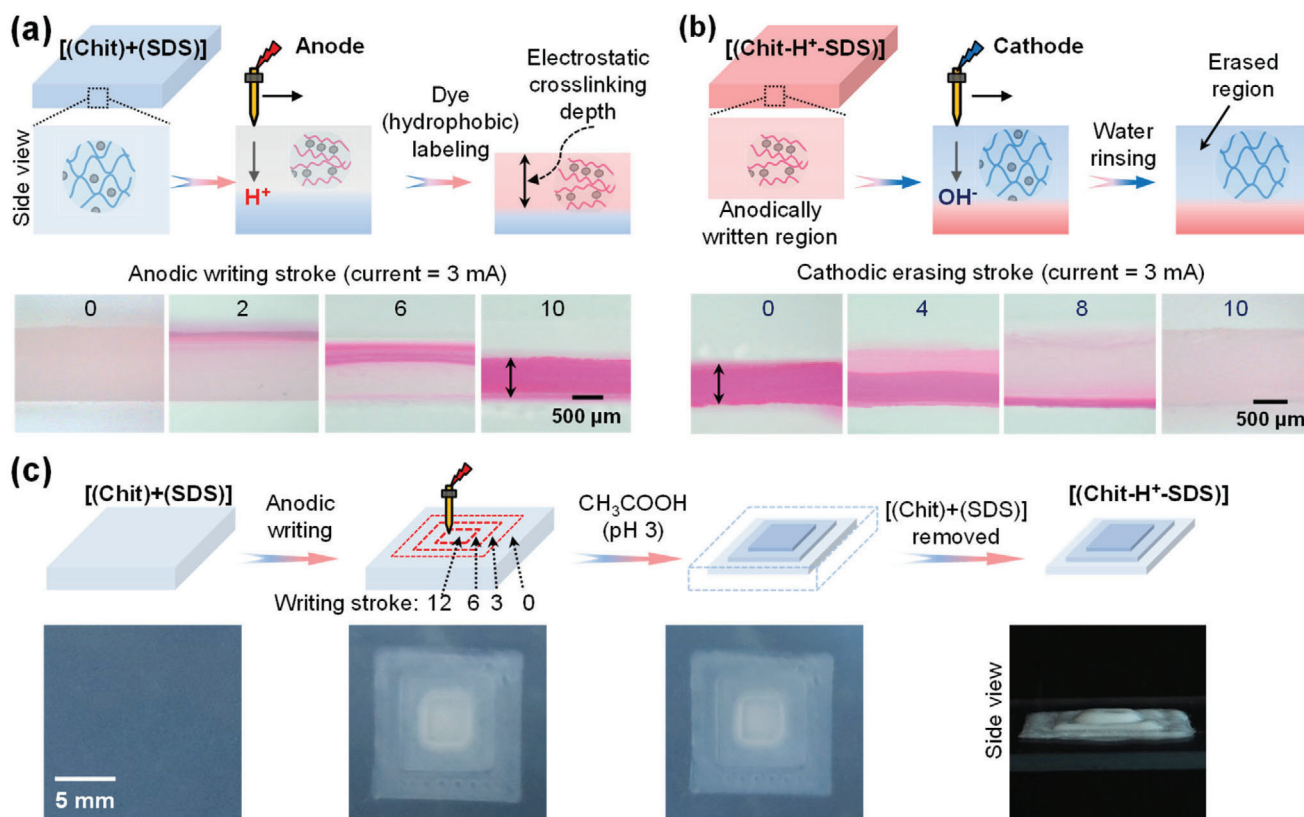


Figure 5. Simple demonstrations of electronic writing for 3D patterning. a) Anodic writing generates an electrostatically crosslinked [(Chit-H⁺)-SDS] region within the [(Chit)+(SDS)] medium. b) The coupling of anodic writing and cathodic erasing can localize the [(Chit-H⁺)-SDS] region at different depths suggesting the possibility that the dynamically responsive [(Chit)+(SDS)] medium can serve as a 3D rewritable memory. c) Schematic and photographs illustrate that the coupling of anodic writing with selective subtraction by acetic acid can create 3D structures.

electrical inputs that are capable of reconfiguring the medium's supramolecular structure also alter its mechanical properties. It is interesting to note that in traditional polymer physics, the mechanical properties can be linked to crosslink density. In our system, it is difficult to precisely define or experimentally measure a crosslink as it is not clear how many sugar residues (or even polysaccharide chains) participate in a crystalline network junction or an SDS crosslink.

2.3. Patterning in Three Dimensions

2.3.1. Potential for Rewritable 3D Memory

The spotting studies in Figures 2a and 3a illustrate that the 2D surface area that is reconfigured is controlled by the electronic inputs. Importantly, these structural reconfigurations occur over three dimensions and this provides the opportunity to create 3D patterns. In an initial study schematically illustrated in Figure 5a, we started with a [(Chit)+(SDS)] medium (2 mm thick, 0.2 M SDS) and performed anodic writing (3 mA, 0.8 mm electrode) for various writing strokes to convert the [(Chit)+(SDS)] medium into [(Chit-H⁺)-SDS]. After anodic writing, we then immersed the written hydrogels into a solution containing the cationic dye Rhodamine B (0.01%) for 10 min and then rinsed the films in DI wa-

ter for 24 h to remove unbound dye molecules and free SDS (Rhodamine B is commonly used dye to detect SDS).^[50] Images of the cross-sections of these films are shown at the bottom of Figure 5a. The first observation in Figure 5a is that anodic writing results in a contraction of the hydrogel which is consistent with previous observations that report the electrostatically crosslinked [(Chit-H⁺)-SDS] network is denser than the [(Chit)+(SDS)] network.^[35] The second observation from Figure 5a is that the electrostatically crosslinked region that is visualized by the Rhodamine is thicker for films that were written with a greater number of writing strokes. These images also indicate that 10 strokes of anodic writing completely reconfigures this 2 mm thick [(Chit)+(SDS)] medium.

Next, we started with 0.6 mm films that were completely reconfigured by anodic writing and stained with Rhodamine, and then we performed cathodic erasing using a different number of erasing strokes. After rinsing, the cross-sections of the films were imaged. As expected, Figure 5b shows the supramolecular structural reconfigurations induced by cathodic erasing: i) lead to an expansion of the film; and ii) start at the surface with the penetration depth progressively increasing with the number of cathodic writing strokes. It should be noted that prolonged exposure to strong acid or base can cause hydrolysis, but we have no evidence that the transient pH excursions induced by electronic writing led to such reactions. For example, Figure S5 (Supporting

Information) shows that multiple cycles of anodic writing and erasing of different patterns can be performed on the same chitosan-SDS medium.

The important implication of the results in Figure 5a,b is that by tailoring the anodic writing and cathodic erasing inputs, it should be possible to precisely localize a reconfigured zone within a 3D hydrogel. Thus, we believe this demonstration experiment suggests the potential for using electronic writing with the dynamically responsive chitosan-SDS medium to create a rewritable 3D memory.

2.3.2. Creating 3D Structure by Electronic Writing and Selective Subtraction

Often, complex 3D structures are fabricated by coupling additive and subtractive steps. Recent studies demonstrate that stimuli-responsive biological polymers provide unique opportunities to create complex hydrogel structure because these polymers offer unique capabilities for selective subtraction.^[51–53] As described in the Supporting Information (Figure S6), we observed that the electrostatically crosslinked [(Chit-H⁺-SDS)] network did not dissolve in acetic acid solutions (≈57 mM; pH 3) that were capable of dissolving the neutral [(Chit)] network that was crosslinked through crystalline network junctions. Thus, such acetic acid solutions could be used for the selective subtraction of electronically written structures.

To demonstrate the coupling of electronic writing with selective subtraction, we performed the experiment illustrated in Figure 5c. Specifically, we anodically patterned a pyramid structure of [(Chit-H⁺-SDS)] into the [(Chit)+(SDS)] medium, rinsed this patterned film for 24 h to remove the free SDS, and then immersed this patterned film into an acetic acid solution (≈57 mM; pH 3) for 5 h to dissolve away the unpatterned regions (i.e., the neutral chitosan [(Chit)]). Photographs in Figure 5c illustrate the crosslinked [(Chit-H⁺-SDS)] pyramid pattern was not dissolved by the acetic acid.

The demonstration in Figure 5c illustrates that the supramolecular structure generated by anodic writing (i.e., the electrostatically crosslinked [(Chit-H⁺-SDS)] network) resists dissolution by acetic acid and this may provide an additional subtractive mechanism for fabricating hydrogel systems with complex structure.^[52–53]

2.4. Conceal and Reveal Information through SDS Structural Transitions

We next demonstrate that information written into the [(Chit)+(SDS)] medium can be concealed and revealed through SDS structural transitions. In initial experiments, NaCl was added to a solution of SDS micelles and a white “precipitate” was observed (see Figure S7a in the Supporting Information). The TEM images in Figure 6a show dramatically different structures appear in SDS solutions (0.2 M) in the presence or absence of NaCl (2 M) and these observations are consistent with previous reports that NaCl can induce SDS to undergo a transition from spherical micelles to worm-like micelles (SDS*).^[54–55]

Figure 6b shows environmental SEM images of a wet film with a written [(Chit-H⁺-SDS)] region and an unwritten

[(Chit)+(SDS)] region. As discussed previously, the [(Chit-H⁺-SDS)] supramolecular state induced by anodic writing is denser and opaque, while the upper-left image in Figure 6b suggests that the SDS micelles within this electrostatically crosslinked region are larger and deformed consistent with molecular modeling studies.^[33,37,40] After immersing this film in an NaCl solution, the SDS micelles in both the written and unwritten areas appear to undergo dramatic structural changes consistent with transitions of spherical micelles into worm-like micelles (SDS*).

One approach to conceal the written patterns is to use salt-induced structural transitions of SDS to obscure the patterns. Experimentally, Figure 6c shows that a “dolphin” pattern was first anodically written (4 strokes, 3 mA) into the [(Chit)+(SDS)] medium. EDS (energy dispersive spectroscopy) imaging of this patterned film shows that elemental sulfur associated with SDS is distributed throughout the patterned and unpatterned regions, while quantitative sulfur line scanning of EDS at the top in Figure 6d shows small differences in sulfur content between the written and unwritten regions.

The patterned film was then immersed in an NaCl solution (2 M) for 5 min, and the middle photograph in Figure 6c shows both the written and unwritten regions became opaque thus obscuring the pattern. EDS line scanning at the middle of Figure 6d shows no significant differences in the sulfur content between the written and unwritten regions which suggests that the pattern is being obscured due to the supramolecular transition of SDS to worm-like micelles. To reveal the obscured pattern, the film was immersed in water for 24 hours to remove NaCl and the free SDS micelles in the unwritten region. The right photograph in Figure 6c shows the previously obscured dolphin pattern is revealed by water-washing, while the EDS analysis shows a significant difference in sulfur content between the patterned region where sulfur is retained (due to SDS’s electrostatic crosslinking with chitosan) and the unpatterned region where sulfur is lost during the water washing step. Video S1 (Supporting Information) shows that a water wash of only 3 min can reveal the pattern and that when a short water wash is used to limit the loss of SDS from the unpatterned region, then the pattern can be repeatedly obscured and revealed by switching the film between a salt solution and water.

A second approach to conceal a written pattern is to make the pattern invisible (evanescent). To illustrate this possibility, Figure 6e shows that we started by anodically writing a dolphin pattern into the [(Chit)+(SDS)] medium. This patterned film was then immersed into water for 24 h to remove free SDS from the unpatterned region (SDS is retained in the written region due to strong electrostatic interactions with chitosan). Next, the patterned film was immersed into a basic solution (0.1 M NaOH) for 5 min and as illustrated by photograph in Figure 6e, the pattern became invisible. Mechanistically, this base treatment neutralizes the chitosan chains in the patterned region thus disrupting its electrostatic crosslinking interactions with SDS micelles (i.e., the patterned [(Chit-H⁺-SDS)] is reconfigured to the [(Chit)+(SDS)] supramolecular state). Although the electrostatic crosslinks have been lost and the pattern cannot be observed, the SDS remains in the patterned region as evidenced by the sulfur mapping in Figure 6f (presumably the pattern has lost its opacity because the SDS micelles have transitioned to small spherical

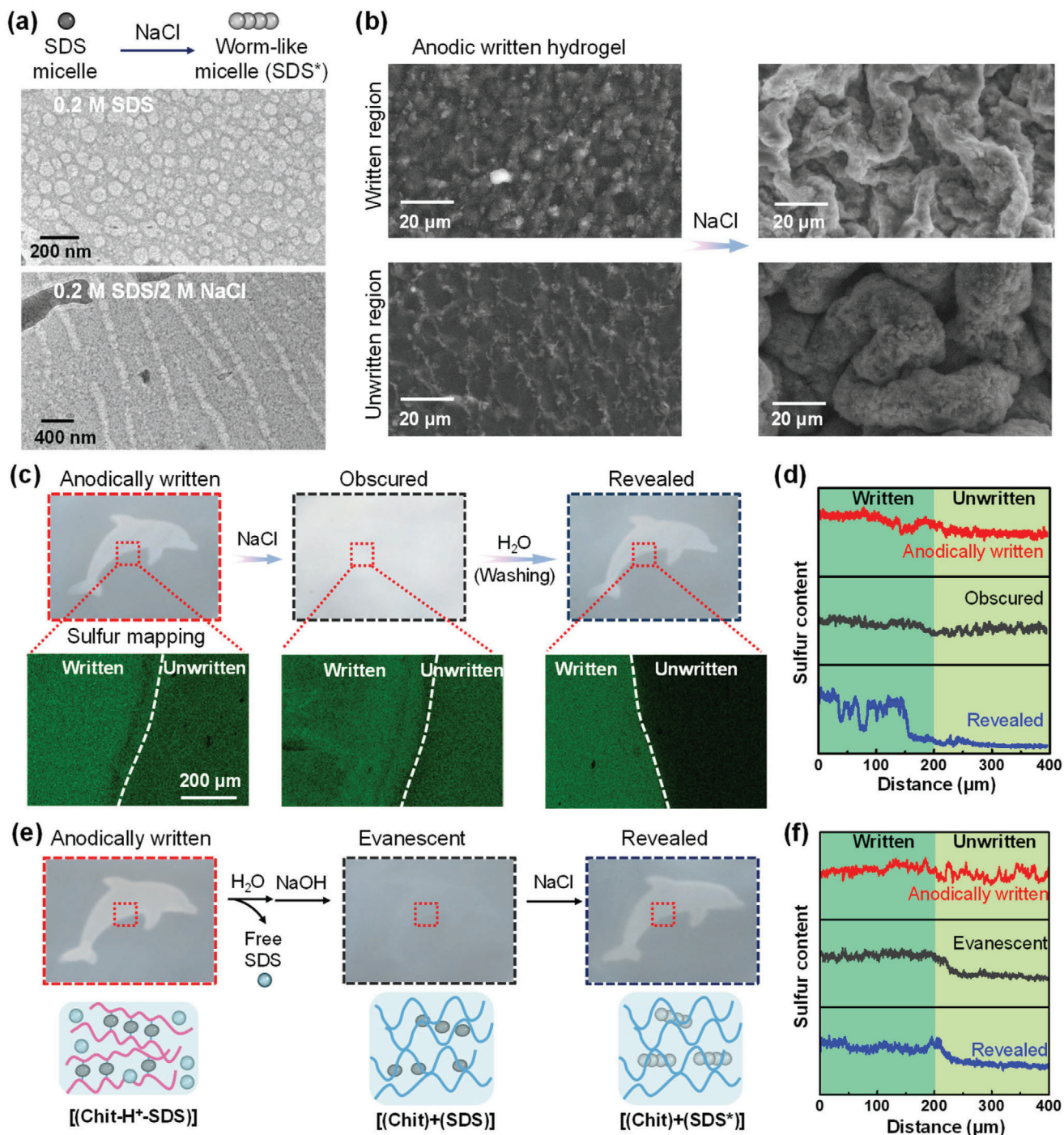


Figure 6. Concealing and revealing patterned information. a) TEM images show NaCl-induced structural transitions of SDS micelles. b) ESEM (environmental SEM) images show the effect of NaCl on the morphology of hydrogel film. c) Patterns written into the hydrogel films can be obscured by salt-induced structural transitions of SDS micelles and revealed by water treatment (Video S1, Supporting Information). d) Sulfur distributions of written and unwritten regions of hydrogel films measured by EDS line scanning. e) Patterns written into the film can be made evanescent (i.e., invisible) by base treatment and the evanescent pattern can be revealed by treatment with salt (Video S2, Supporting Information). Sulfur mapping images are shown in Figure S7b (Supporting Information). f) Sulfur distribution of the written but evanescent region and the unwritten region of hydrogel films EDS measured by line scanning.

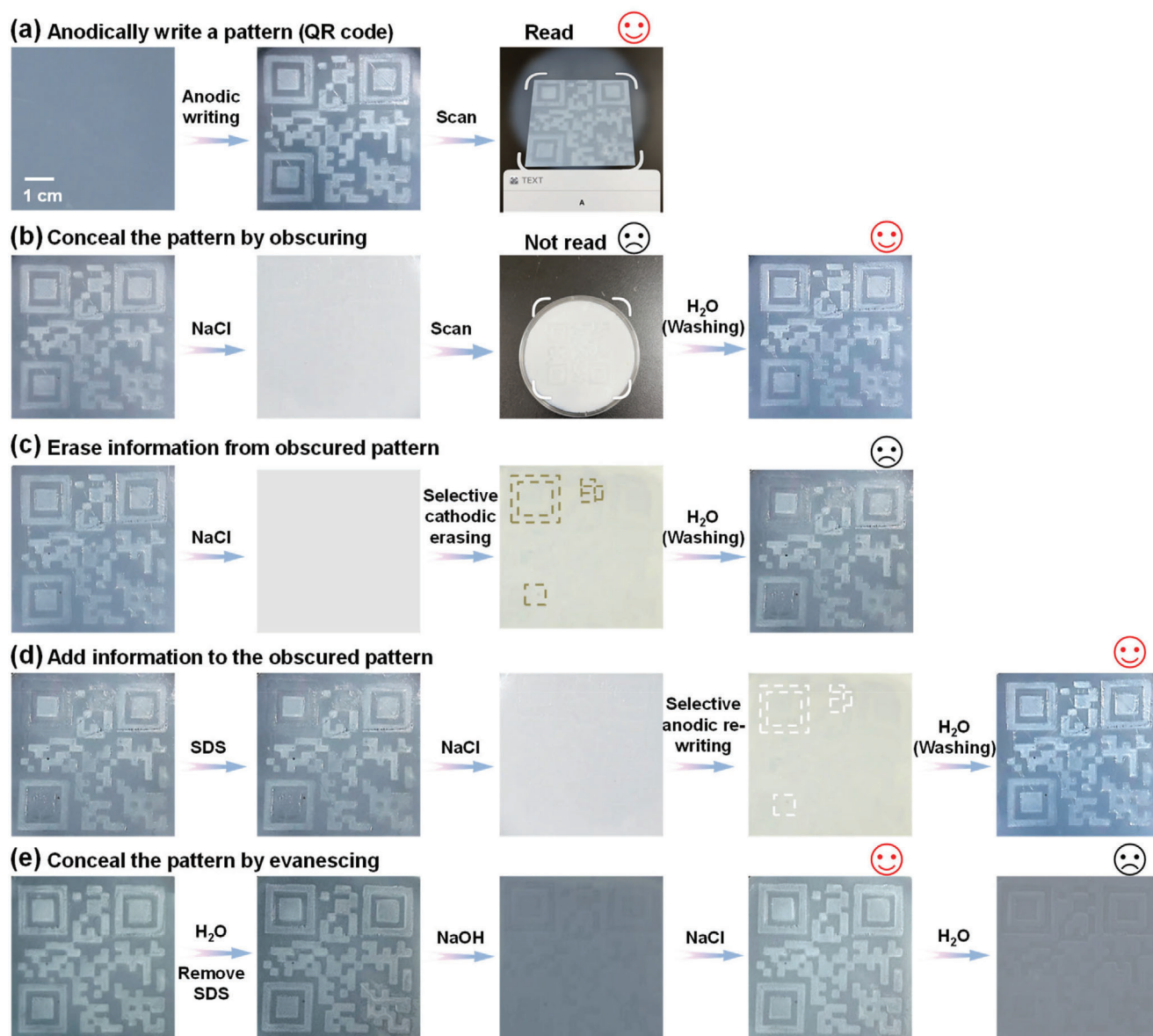


Figure 7. Capability of chitosan-SDS as an informational material. a) Anodically patterned QR code is machine-readable by a cellphone. b) The QR code can be concealed (by obscuring) or revealed using salt or water to induce transitions in SDS's micellar structure. A concealed QR code can be electronically modified to: c) delete information by cathodic erasing (1 mA, 4 strokes); or d) add information by anodic re-writing (1 mA, 4 strokes). e) The QR code can be concealed (by evanescence) and revealed by simple water/salt treatments.

micelles). This evanescent pattern can then be revealed by immersing the film in 2 M NaCl for 5 min to induce the SDS to transition into worm-like micelles that confer opacity to the pattern. Video S2 (Supporting Information) shows the evanescing and revealing of the pattern is also reversible: if the water washing is short to limit the loss of SDS from the evanescent pattern, then the pattern can be repeatedly revealed and concealed by switching the film between a salt solution and water.

In sum, electrode writing and erasing can create patterns in the [(Chit)+(SDS)] medium by locally inducing structural transitions in chitosan's supramolecular state, and Figure 6 shows these patterns can be concealed and revealed by inducing structural transitions in SDS's supramolecular state.

2.5. Chitosan-SDS as A Dynamically Responsive Information Storage Medium

As a proof-of-concept demonstration, we show that the dynamically responsive [(Chit)+(SDS)] medium can be used to write, store, conceal, and manipulate machine-readable information in a quick response (QR) code. Experimentally, **Figure 7a** shows that the QR code for the letter "A" was anodically written (4 strokes, 1 mA) into the [(Chit)+(SDS)] medium, and this written QR code could be read by a standard cellphone app (see Video S3, Supporting Information). This result illustrates that the information in an electronically written 2D pattern is machine-readable and correctly decoded.

Figure 7b shows that when the patterned medium was immersed in a salt solution (2 M NaCl; 5 min) the pattern was obscured, and the information in this obscured pattern could no longer be read by the cellphone. If this film was immersed in water the obscured pattern could be revealed and correctly read by the cellphone. If the water washing step was short (e.g., 3 min), the pattern could be repeatedly obscured and revealed by salt and water treatments (see Video S4, Supporting Information).

Figure 7c shows that a concealed pattern can be manipulated by cathodic erasing to delete information. Experimentally, the patterned film was first immersed in a salt solution to conceal (i.e., obscure) the QR code, and then a portion of the pattern was deliberately modified by cathodic erasing (1 mA, 4 strokes). After water washing (24 h), the obscured pattern is revealed to have been modified to delete information. This modified pattern could no longer be detected as a valid QR code by the cellphone (see Video S5 in the Supporting Information). Thus, cathodic erasing could delete information from the pattern even when the pattern was being obscured.

Figure 7d shows that a concealed pattern can be manipulated by anodic writing to add information. Experimentally, we used the selectively erased patterned film in Figure 7c and first immersed this film in 0.2 M SDS for 1 h to allow SDS micelles to penetrate into the unpatterned and erased regions, after which the film was transferred to a salt solution (2 M, 5 min) to obscure the pattern. Anodic re-writing (1 mA, 4 strokes) was then performed on the previously erased regions to restore the QR code. After revealing the pattern by immersing the film in water, the restored QR code could again be observed and read by the cellphone (see Video S6, Supporting Information). Importantly, Video S6 (Supporting Information) shows that this patterned QR code could not be removed by immersion in water because of the strong electrostatic interactions between SDS and chitosan in the patterned $[(\text{Chit}-\text{H}^+-\text{SDS})]$ regions.

Finally, Figure 7e shows the patterned QR code can be concealed evanescently. First, the film patterned with the QR code was washed with water for 24 h to remove free SDS in the unpatterned regions (the electrostatically crosslinked SDS in the written regions is retained). Then the film was immersed in a base solution (0.1 M NaOH, 5 min) to convert the supramolecular structure in the patterned region from $[(\text{Chit}-\text{H}^+-\text{SDS})]$ to $[(\text{Chit})+(\text{SDS})]$. After this base treatment, Figure 7e shows the patterned region is no longer visible (i.e., it is being concealed evanescently). To reveal this evanescent pattern, the film was immersed in a salt solution (NaCl 2 M, 5 min) that caused in the patterned region to become opaque and reveal the QR code and enable machine-reading by the cellphone. Video S7 (Supporting Information) shows that the patterned film can be reversibly concealed by evanescence and revealed by short treatments with water (e.g., 5 min) and salt (2 M NaCl, 3 min). However, the evanescent pattern is not stable but can be removed by prolonged water washing.

3. Conclusions

We prepared a dynamically responsive medium from two stimuli-responsive bio-derived self-assembling components and demonstrate that it can be patterned electronically. Chitosan is derived by the de-acetylation of chitin to form a polymer rich

in glucosamine residues that have two stable and pH-dependent protonation states. The residue-level protonation states control chitosan's supramolecular structure. SDS is an anionic surfactant derived from lauryl alcohol that self-associates to form micelles that can undergo reversible NaCl-induced morphological transitions from small globular micelles in the absence of salt to long worm-like micelles at high NaCl. Patterning relies on an electrode "pen" to impose mild (≈ 10 V) transient inputs that induce changes in the subtle physical interactions that are responsible for the individual components to self-assemble and for the individual components to interact with each other.

From an informational materials perspective, there are several interesting features of this work. First, this dynamically responsive medium transduces transient electronic inputs into responses in supramolecular structure. Thus, this medium provides a bridge between the electronic logic of technology and the molecular logic of biology. Second, patterning of the dynamically responsive medium requires that the transiently imposed electrical inputs induce structural transitions that persistent over time. The two supramolecular states ($[(\text{Chit})+(\text{SDS})]$ and $[(\text{Chit}-\text{H}^+-\text{SDS})]$) can persist in adjacent regions because each state is stabilized by structure-induced shifts in chitosan's pKa. Third, electronic patterning enlists convenient and precisely controllable top-down cues to induce bottom-up self-assembly. Because the resulting supramolecular structures are held in place by reversible physical interactions, the patterns can be modified to update the information, while the medium can be erased and rewritten with new information. Fourth, the reversible transitions in SDS's supramolecular structure are integral to the medium's optical properties that allow the patterns to be observed or concealed either by obscuring the pattern or making it invisible (evanescent). In summary, we believe these studies further illustrate the potential of bio-derived self-assembling components to yield high-performance, dynamically responsive, and sustainable materials systems.

4. Experimental Section

Materials: Chitosan ($M_w = 4.06 \times 10^5$ g mol⁻¹, deacetylation degree 85%) was purchased from Tokyo Chemical Industry Co., Ltd (TCI, Shanghai). Hydrochloric acid (HCl), sodium hydroxide (NaOH), sodium chloride (NaCl), and sodium dodecyl sulfate (SDS) were purchased from Sinopharm Chemical Reagent Co., Ltd (China). All the reagents were used as received without further purification. Platinum (Pt) wires were obtained from commercial resources in China.

Preparation of Chitosan $[(\text{Chit})]$ Film and Reaction Solutions: A predetermined amount of chitosan powder was dissolved in HCl solution (1.25%; v/v) to prepare chitosan solution (3%; w/v). After mechanical stirring overnight, the pH of the chitosan solution was adjusted to pH 5–6 by adding chitosan/water mixture (3%, w/v) to minimize salt (mainly NaCl) content, which can dramatically affect structure/properties of the prepared hydrogel.^[32] Then the chitosan solution was poured into a petri dish to a thickness of ≈ 1 mm and set aside to remove bubbles. The chitosan $[(\text{Chit})]$ film was formed by immersing the chitosan solution in 1 M NaOH for 2 h, followed by washing with deionized water to remove excess base (i.e., until the rinse water was neutral). The chitosan film has a water content of $96.5 \pm 0.2\%$. SDS, NaOH, NaCl solutions of different concentrations were prepared by dissolving corresponding reagent powder in deionized water.

Anodic Writing and Cathodic Erasing: The $[(\text{Chit})]$ film was immersed in 0.2 M SDS solution for 1 h to obtain $[(\text{Chit})+(\text{SDS})]$ medium, during which SDS was diffused and dispersed throughout the chitosan film. Two

platinum electrodes were respectively connected with the anode and cathode of the Digital Source-meter (2450, Keithley, USA). One of the platinum electrodes was used as electrode pen for anodic writing or cathodic erasing, and its precise movement was controlled by an auto-mechanical arm (Ultimaker 2 Go, Hesheng, China) with a writing speed of 5 mm s^{-1} . Cura software (Ultimaker) was used to design the anodic writing/cathodic erasing template to regulate the moving trace of the electrode pen. Electrostatic crosslinking of chitosan and SDS on [(Chit)+(SDS)] medium was induced by anodic writing and [(Chit-H⁺-SDS)] film was obtained. Cathodic erasing was carried out on [(Chit-H⁺-SDS)] film, destroying the electrostatic crosslinking of chitosan and SDS.

Characterizations: The absorbance of the films was measured by UV spectrometer (UV-2700, Shimadzu, Japan) in the wavelength range of 390–800 nm. The morphology of wet films was examined by environmental scanning electron microscope (ESEM, Quanta200, FEI, Holland). The morphology of dry films was obtained by lyophilizing in a freeze-dryer (FreeZone, Labconco, USA) and examined with a field emission scanning electron microscope (FE-SEM, Zeiss SIGMA, Carl Zeiss, UK). The contents of C, N, and S elements of films were determined by an element analyzer (Vario EL III, Elementar, Germany). Wide angle X-ray diffraction measurements were performed on a diffractometer (D8-Advance, Bruker, USA) in the 2θ range of $5\text{--}60^\circ$ with Cu K α radiation source at 40 kV and 40 mA. The FT-IR spectra were measured by a Nicolet 5700 spectrometer (Thermo Fisher, USA) in the wavenumber range of $500\text{--}4000 \text{ cm}^{-1}$. A thermogravimetric analyzer (TGA2/DSC3, Mettler Toledo Co., Ltd., Germany) was used to analyze the thermal stability of the films, with a temperature range of $30\text{--}600^\circ\text{C}$ and a heating rate of $10^\circ\text{C min}^{-1}$. A Raman imaging microscope (XploRA plus, HORIBA Jobin Yvon, France) was used to measure Raman spectroscopy and spatial Raman mapping. The wavelength of the excitation laser was 532 nm and the mapping area ($10 \mu\text{m} \times 10 \mu\text{m}$) was scanned with a spatial resolution of 500 nm. The mechanical properties of different films were characterized by tensile test on universal electronic testing machine (CMT6350, SANS, China) at a stretching rate of 10 mm min^{-1} . The images of spherical SDS micelles and worm-like SDS micelles (SDS*) were recorded on transmission electron microscope (JEM-2100, JEOL, Japan). Distribution of S element of the films were obtained by EDS (energy dispersive spectroscopy) on a field emission electron probe micro-analyzer (JXA-8530F Plus, JEOL, Japan).

Supporting Information

Supporting Information is available from the Wiley Online Library or from the author.

Acknowledgements

This work was supported by the National Natural Science Foundation of China (22275141; 22075215), the National Science Foundation of the US (CBET 1932963), and the Betty and Gordon Moore Foundation.

Conflict of Interest

The authors declare no conflict of interest.

Data Availability Statement

The data that support the findings of this study are available from the corresponding author upon reasonable request.

Keywords

chitosan hydrogels, electrofabrication, information storage, reconfigurable materials, sodium dodecylsulfate, supramolecular structures

Received: March 5, 2023
Revised: April 11, 2023
Published online: May 14, 2023

- [1] F. Sheehan, D. Sementa, A. Jain, M. Kumar, M. Tayarani-Najjaran, D. Kroiss, R. V. Ulijn, *Chem. Rev.* **2021**, *121*, 13869.
- [2] M. S. Ganewatta, Z. K. Wang, C. B. Tang, *Nat. Rev. Chem.* **2021**, *5*, 753.
- [3] A. Brito, S. Kassem, R. L. Reis, R. V. Ulijn, R. A. Pires, I. Pashkuleva, *Chem* **2021**, *7*, 2943.
- [4] L. Stefan, D. Monchaud, *Nat. Rev. Chem.* **2019**, *3*, 650.
- [5] J. S. Kahn, Y. W. Hu, I. Willner, *Accounts Chem. Res.* **2017**, *50*, 680.
- [6] L. Petridis, J. C. Smith, *Nat. Rev. Chem.* **2018**, *2*, 382.
- [7] K. Y. Zhu, H. Merzendorfer, W. Q. Zhang, J. Z. Zhang, S. Muthukrishnan, in *Annu. Rev. Entomol.*, Vol. 61 (Ed: M. R. Berenbaum), Annual Reviews, Palo Alto, **2016**, pp. 177–196.
- [8] M. Benitez, V. Hernandez-Hernandez, S. A. Newman, K. J. Niklas, *Front Plant Sci* **2018**, *9*, 16.
- [9] S. A. Newman, *Science* **2012**, *338*, 217.
- [10] S. A. Newman, R. Bhat, *Int. J. Dev. Biol.* **2009**, *53*, 693.
- [11] S. Kassem, R. V. Ulijn, *ChemSystemsChem* **2023**, *5*, 202200049.
- [12] K. Lou, Z. Q. Hu, H. W. Zhang, Q. Y. Li, X. F. Ji, *Adv. Funct. Mater.* **2022**, *32*, 2113274.
- [13] C. T. Yu, H. L. Guo, K. P. Cui, X. Y. Li, Y. N. Ye, T. Kurokawa, J. P. Gong, *Proc. Natl. Acad. Sci. USA* **2020**, *117*, 18962.
- [14] W. Lu, M. Q. Si, X. X. Le, T. Chen, *Accounts Chem. Res.* **2022**, *55*, 2291.
- [15] C. T. Yu, K. P. Cui, H. L. Guo, Y. N. Ye, X. Y. Li, J. P. Gong, *Macromolecules* **2021**, *54*, 9927.
- [16] L. De Smet, K. Belal, A. Vebr, J. Lyskawa, F. Stoffelbach, R. Hoogenboom, P. Woisel, *ACS Mater. Lett.* **2023**, *5*, 235.
- [17] X.-X. Le, W. Lu, J. He, M. J. Serpe, J.-W. Zhang, T. Chen, *Sci. China Mater* **2019**, *62*, 831.
- [18] X. X. Le, H. Shang, H. Z. Yan, J. W. Zhang, W. Lu, M. J. Liu, L. P. Wang, G. M. Lu, Q. J. Xue, T. Chen, *Angew. Chem.-Int. Edit.* **2021**, *60*, 3640.
- [19] J. Li, M. Tian, H. Xu, X. Ding, J. Guo, *Part. Part. Syst. Character.* **2019**, *36*, 1900346.
- [20] Y. Sun, X. X. Le, S. Y. Zhou, T. Chen, *Adv. Mater.* **2022**, *34*, 2201262.
- [21] J. Hou, H. Zhang, B. Su, M. Li, Q. Yang, L. Jiang, Y. Song, *Chem Asian J* **2016**, *11*, 2680.
- [22] J. Y. Yan, G. Y. Pan, W. J. Lin, Z. L. Tang, J. H. Zhang, J. X. Li, W. P. Li, X. F. Lin, H. S. Luo, G. B. Yi, *Chem. Eng. J.* **2023**, *451*, 12.
- [23] H. H. Lu, B. Y. Wu, X. X. Le, W. Lu, Q. Yang, Q. Q. Liu, J. W. Zhang, T. Chen, *Adv. Funct. Mater.* **2022**, *32*, 2206912.
- [24] D. Y. Lou, Y. J. Sun, J. Li, Y. Y. Zheng, Z. P. Zhou, J. Yang, C. X. Pan, Z. K. Zheng, X. D. Chen, W. Liu, *Angew. Chem.-Int. Edit.* **2022**, *61*, e202117066.
- [25] Q. Wang, Z. Qi, Q. M. Wang, M. Chen, B. Y. Lin, D. H. Qu, *Adv. Funct. Mater.* **2022**, *32*, 2208865.
- [26] M. Li, H. L. Lu, X. Y. Wang, Z. S. Wang, M. H. Pi, W. Cui, R. Ran, *Small* **2022**, *18*, 2205359.
- [27] H. H. Lu, B. Y. Wu, X. X. Yang, J. W. Zhang, Y. K. Jian, H. Z. Yan, D. C. Zhang, Q. J. Xue, T. Chen, *Small* **2020**, *16*, 2005461.
- [28] Y. Ou, M. Tian, *J. Mat. Chem. B* **2021**, *9*, 7955.
- [29] E. Kim, Y. Xiong, Y. Cheng, H. C. Wu, Y. Liu, B. H. Morrow, H. Ben-Yoav, R. Ghodssi, G. W. Rubloff, J. N. Shen, W. E. Bentley, X. W. Shi, G. F. Payne, *Polymers* **2015**, *7*, 1.
- [30] Y. Liu, E. Kim, R. Ghodssi, G. W. Rubloff, J. N. Culver, W. E. Bentley, G. F. Payne, *Biofabrication* **2010**, *2*, 022002.
- [31] H. M. Yi, L. Q. Wu, W. E. Bentley, R. Ghodssi, G. W. Rubloff, J. N. Culver, G. F. Payne, *Biomacromolecules* **2005**, *6*, 2881.

- [32] Y. Liu, B. Zhang, K. M. Gray, Y. Cheng, E. Kim, G. W. Rubloff, W. E. Bentley, Q. Wang, G. F. Payne, *Soft Matter* **2013**, 9, 2703.
- [33] C. C. Tsai, G. F. Payne, J. N. Shen, *Chem. Anal. Biol. Fate: Polynucl. Aromat. Hydrocarbons, Int. Symp., 5th* **2018**, 30, 8597.
- [34] H. M. He, J. Y. Li, X. D. Cao, C. S. Ruan, Q. Feng, H. Dong, G. F. Payne, *ACS Appl Bio Mater* **2018**, 1, 1695.
- [35] H. He, X. Cao, H. Dong, T. Ma, G. F. Payne, *Adv. Funct. Mater.* **2017**, 27, 1605665.
- [36] S. Jiang, C. D. Qiao, X. J. Wang, Z. W. Li, G. H. Yang, *RSC Adv.* **2022**, 12, 3969.
- [37] B. H. Morrow, G. F. Payne, J. Shen, *J. Am. Chem. Soc.* **2015**, 137, 13024.
- [38] L. Tang, L. Gong, Y. Xu, S. Wu, W. Wang, B. Zheng, Y. Tang, D. Zhang, J. Tang, J. Zheng, *ACS Appl. Nano Mater.* **2022**, 5, 1348.
- [39] J. Chen, L. Xu, X. Lin, R. Chen, D. Yu, W. Hong, Z. Zheng, X. Chen, *J. Mater. Chem. C* **2018**, 6, 7767.
- [40] S. Gotla, C. Tong, S. Matysiak, *ACS Appl. Nano Mater* **2022**, 5, 6463.
- [41] P. Pal, A. Pal, *Int. J. Biol. Macromol.* **2017**, 104, 1548.
- [42] C. Yang, X. W. Shi, H. B. Deng, Y. M. Du, *ACS Appl. Mater. Interfaces* **2022**, 14, 6251.
- [43] X. Y. Zhu, C. Yang, Y. H. Jian, H. B. Deng, Y. M. Du, X. W. Shi, *Carbohyd. Polym.* **2022**, 276, 118759.
- [44] K. Yan, F. Y. Ding, W. E. Bentley, H. B. Deng, Y. M. Du, G. F. Payne, X. W. Shi, *Soft Matter* **2014**, 10, 465.
- [45] S. Wu, K. Yan, Y. A. Zhao, C. C. Tsai, J. Shen, W. E. Bentley, Y. Chen, H. B. Deng, Y. M. Du, G. F. Payne, X. W. Shi, *Adv. Funct. Mater.* **2018**, 28, 1803139.
- [46] D. Zhao, J. C. Huang, Y. Zhong, K. Li, L. N. Zhang, J. Cai, *Adv. Funct. Mater.* **2016**, 26, 6279.
- [47] D. D. Xu, J. C. Huang, D. Zhao, B. B. Ding, L. N. Zhang, J. Cai, *Adv. Mater.* **2016**, 28, 5844.
- [48] C. Yang, X. W. Shi, L. H. Qi, X. Y. Zhu, J. Tong, H. B. Deng, Y. M. Du, *ACS Appl. Mater. Interfaces* **2021**, 13, 36538.
- [49] J. Zou, S. Q. Wu, J. Chen, X. J. Lei, Q. H. Li, H. Yu, S. Tang, D. D. Ye, *Adv. Mater.* **2019**, 31, 1904762.
- [50] F. J. Li, A. P. Zhu, X. L. Song, L. J. Ji, J. Wang, *Int. J. Pharm.* **2013**, 453, 506.
- [51] H. Wen, J. Li, G. F. Payne, Q. Feng, M. Liang, J. Chen, H. Dong, X. Cao, *Biofabrication* **2020**, 12, 035007.
- [52] H. X. Su, Q. T. Li, D. G. Li, H. F. Li, Q. Feng, X. D. Cao, H. Dong, *Mater. Horiz.* **2022**, 9, 2393.
- [53] Q. Feng, D. G. Li, Q. T. Li, X. D. Cao, H. Dong, *Bioact Mater* **2022**, 9, 105.
- [54] K. Schafer, H. B. Kolli, M. K. Christensen, S. L. Bore, G. Diezemann, J. Gauss, G. Milano, R. Lund, M. Cascella, *Angew. Chem.-Int. Edit.* **2020**, 59, 18591.
- [55] G. V. Jensen, R. Lund, J. Gummel, T. Narayanan, J. S. Pedersen, *Angew. Chem.-Int. Edit.* **2014**, 53, 11524.